

Ultra-high-resolution observations of Ca K line variations in the β Pictoris disc

I. A. Crawford,^{1,2} J. Spyromilio,² M. J. Barlow,¹ F. Diego¹ and A. M. Lagrange³

¹Department of Physics and Astronomy, University College London, Gower Street, London WC1E 6BT

²Anglo-Australian Observatory, PO Box 296, Epping, New South Wales 2121, Australia

³Groupe d'Astrophysique de Grenoble, Université J. Fourier, BP 53X, F-38041 Grenoble Cédex, France

Accepted 1993 December 6. Received 1993 November 17

ABSTRACT

We present observations of the β Pictoris circumstellar Ca II K line, obtained with the new Ultra-High-Resolution facility (UHRF) at the Anglo-Australian Telescope. The resolving power was $R \geq 900\,000$, and these data therefore comprise the highest resolution observations yet obtained of this object. Observations were obtained on three nights in 1993 (May 11, August 26 and August 29), and significant temporal variability was observed, including previously unobserved changes in the profile of the main circumstellar component.

Key words: line: profiles – circumstellar matter – stars: individual: β Pic.

1 INTRODUCTION

The bright ($V=3.85$) southern A5V star β Pictoris is the best-known of the main-sequence ‘Vega-excess’ stars found by the *IRAS* survey to exhibit circumstellar dust emission (Aumann 1984). Optical coronagraphic imaging by Smith & Terrile (1984) revealed the dust to form an edge-on disc, and this disc has been imaged in great detail at optical wavelengths (Smith & Terrile 1984; Paresce & Burrows 1987; Gledhill, Scarrott & Wolstencroft 1991; Golimowski, Durrance & Clampin 1993; Lecavelier des Etangs et al. 1993). The edge-on geometry of the disc lends itself to study by absorption-line spectroscopy against the stellar photosphere, and a gaseous component was first detected in this way by Hobbs et al. (1985). Subsequent observations conducted with a velocity resolution of about 3 km s^{-1} (e.g. Ferlet, Hobbs & Vidal-Madjar 1987; Lagrange-Henri et al. 1992, and references therein) have found strong temporal variations in the red wing of the circumstellar Ca K line. Similar variations are found to occur in the UV line profiles of circumstellar ions observed by *IUE* (Kondo & Bruhweiler 1985; Lagrange, Ferlet & Vidal-Madjar 1987) and the Goddard High Resolution Spectrometer (GHRS) of the *Hubble Space Telescope* (Boggess et al. 1991). There is now considerable evidence that the bulk of the gas lies within 1–2 au of the star (Kondo & Bruhweiler 1985; Hobbs et al. 1988; Boggess et al. 1991), and the fact that the strongest line profile variations are all redshifted with respect to the stellar radial velocity has led to the suggestion (Lagrange-Henri, Vidal-Madjar & Ferlet 1988; Beust et al. 1989, 1990) that they are caused by solid, kilometre-sized bodies evaporating as they fall towards the star on parabolic orbits.

Here we report ultra-high-resolution observations of the circumstellar Ca K line obtained with the new Ultra-High-

Resolution Facility (UHRF) at the AAT. This instrument, an echelle spectrograph capable of resolving powers of up to $R \approx 10^6$, is currently the highest resolution optical astronomical spectrograph in the world (Barlow et al., in preparation; Diego et al., in preparation), and it has enabled us to resolve the circumstellar line profiles fully for the first time.

2 OBSERVATIONS AND DATA REDUCTION

Observations were obtained on three nights: 1993 May 11, August 26 and August 29. The spectra were obtained with the aid of a newly implemented 35-slice confocal image slicer (Diego 1993), and the detector was the AAO Blue Thomson CCD (1024×1024 19- μm pixels). In order to reduce the CCD readout noise, 2-pixel on-chip binning was employed perpendicular to the dispersion direction. The exposure time was 1800 s in each case, and approximately 500 counts (e^-) were obtained at the bottom of the very strong stellar Ca K line (which acts as the local continuum for the circumstellar absorption). The spectra were extracted from the CCD images using the FIGARO data reduction package (Shortridge 1988).

Wavelength calibration was provided by means of a Th–Ar lamp. Linear fits to between five and seven (mostly very weak, and previously unidentified) Th–Ar lines within the 1.8- \AA spectral coverage of the detector gave rms residuals of $(6 \pm 1) \times 10^{-4} \text{ \AA}$ (0.05 km s^{-1}).

2.1 Spectral resolution

The instrumental resolution was determined from the observed profile of a stabilized He–Ne laser. The laser profiles obtained on the nights of the present observations yielded velocity resolutions in the range 0.303 to 0.332

km s^{-1} (FWHM), corresponding to resolving powers in the range 990 000 to 904 000, respectively. Thus all the circumstellar lines reported here have been fully resolved.

2.2 Background removal

The image slicer produces a very long (20 mm) slit composed of 35 individual slices (Diego 1993), which is then compressed by about a factor of 20 by means of a cylindrical lens placed immediately in front of the detector. This arrangement greatly increases the efficiency of the instrument, but makes it impossible to measure directly the scattered light from the inter-order region (all light entering the lens, order and inter-order, is focused on to a 1-mm wide strip down the centre of the detector).

At present, the only sure way to determine the amount of scattered light present in UHRF spectra is to measure the residual intensity in the core of a fully saturated absorption line. Fortunately for the present study, there is considerable evidence that the main circumstellar Ca K component towards β Pic is indeed fully saturated.

(i) Within the noise, the core of this component is flat, which is characteristic of fully saturated absorption lines.

(ii) Comparison of the UHRF Ca K profile with lower resolution (5.3 km s^{-1}) UCLES spectra (obtained on 1992 December 31) strongly suggests that the main circumstellar component is fully saturated. Specifically, if the UHRF spectrum is degraded to the UCLES resolution, agreement between the two profiles is obtained under the assumption that the main component reaches zero intensity in the core, but not if the line profile is as measured in the raw spectrum (≈ 19 per cent residual intensity in the core relative to the local continuum).

(iii) The UCLES spectra included both the K and H lines of Ca II, thus making it possible to determine the degree of saturation by measuring the doublet ratio. The equivalent widths of the K and H lines were found to be 112 ± 10 and

$100 \pm 8 \text{ m}\text{\AA}$, respectively, giving a doublet ratio of 1.12 ± 0.13 . Following Somerville (1988), we see that the upper limit to the doublet ratio (1.25) corresponds to a minimum optical depth in the core of the K line of $\tau_c = 5.90$, or a maximum residual intensity of 2.7×10^{-3} (a doublet ratio of 1.12 would imply a residual intensity of only 4×10^{-10}). Thus the doublet ratios strongly imply that there is negligible residual flux in the core of the main component of the circumstellar Ca K line.

Thus, in what follows, we assume that the main circumstellar component is fully saturated, and that its core marks the true zero level of the residual intensity scale. We note that no fully saturated *interstellar* Ca II K line is currently known, in stark contrast to this circumstellar component.

3 DISCUSSION

Fig. 1 shows the three spectra plotted on a heliocentric velocity scale. For ease of comparison, all have been normalized to unit relative intensity at zero heliocentric velocity. The star has a radial velocity of $+20 \text{ km s}^{-1}$, and the circumstellar absorption occurs at the base of the stellar Ca K line centred on this velocity. A number of qualitative observations may immediately be made concerning the spectra shown in Fig. 1.

(i) The blue wing of the stellar line is found to be identical for all three spectra. In the red wing, however, very strong line profile variations are observed, consistent with the results of Ferlet et al. (1987) and Lagrange-Henri et al. (1992).

(ii) On May 11 a very strong (almost saturated) circumstellar component was present at a heliocentric velocity of approximately $+33 \text{ km s}^{-1}$, but this was absent during the August observations. On the other hand, while the approximately symmetrical shape of the stellar K line was preserved in May, by August the red wing had become severely

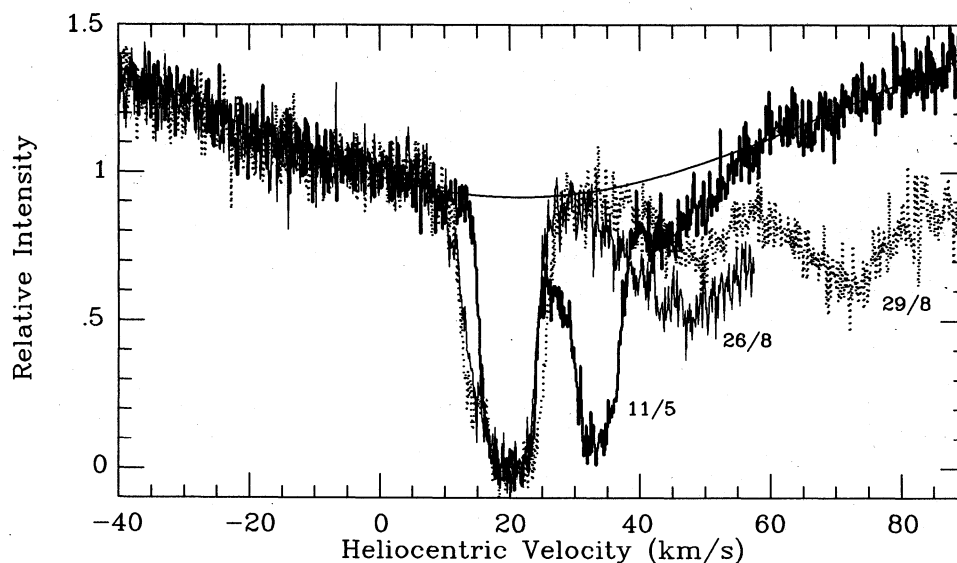


Figure 1. UHRF observations of the β Pictoris circumstellar Ca II K components. The three sets of observations have all been normalized to unit relative intensity at zero heliocentric velocity, and plotted with different line types; the dates of observation are indicated on the plot. The smooth curve is a Gaussian fit to the photospheric K line.

depressed as a result of very broad circumstellar absorptions extending out to a heliocentric velocity of at least $+90 \text{ km s}^{-1}$.

(iii) Small, but significant, variations were found in the profile of the main circumstellar component at $+20 \text{ km s}^{-1}$. Specifically, the two profiles obtained in August exhibit absorption in the blue wing of this component which was absent on May 11. Moreover, while the red wings of the main component were found to coincide on May 11 and August 26, additional absorption was clearly present on August 29. To our knowledge, this is the first time that such variability in the main component has been clearly observed.

In order to obtain the column densities and velocity dispersions of the various circumstellar components, theoretical line profiles were calculated using the line profile modelling routines incorporated into the `DIPO` data analysis program (Howarth & Murray 1988). The theoretical profiles are shown superimposed on the observed profiles in Fig. 2 (where the photospheric K line has been removed by dividing out the smooth curve indicated in Fig. 1). The resulting line profile parameters are given in Table 1, and identify the *minimum* number of discrete absorption components that

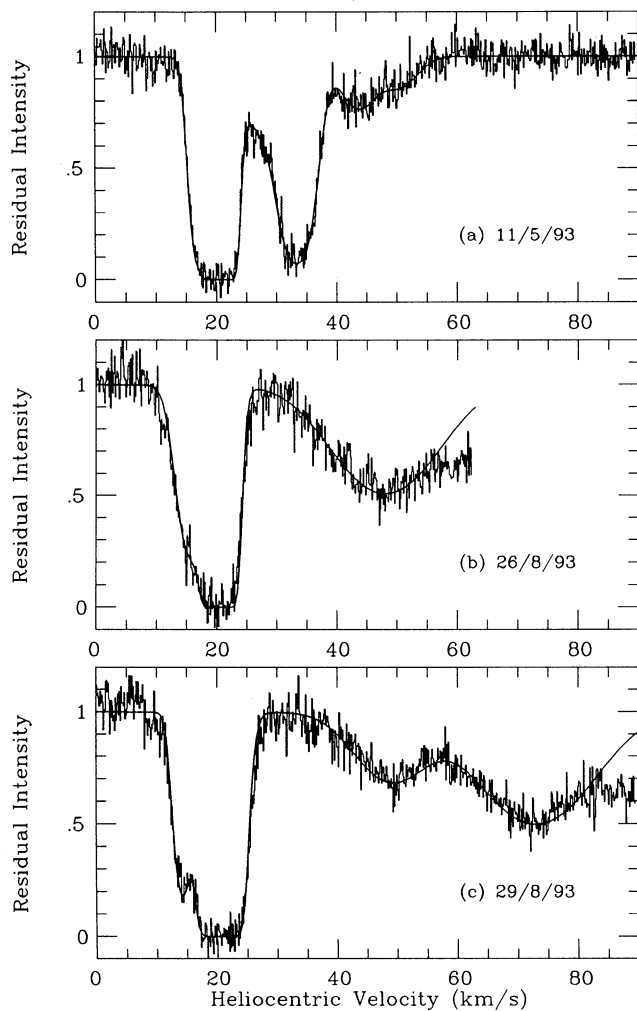


Figure 2. The circumstellar Ca K line profiles observed on the three dates. The photospheric line has been removed by dividing by the Gaussian fit shown in Fig. 1. The smooth curves are theoretical line profiles with the parameters given in Table 1.

are required to fit the observed profiles. Additional unresolved components may well be present, and the variations found in the profile of the main component certainly suggest the presence of substructure. A higher signal-to-noise ratio might also reveal that the ‘broad’ redshifted components observed in August contain narrower sub-components.

We find the main (saturated) component to have a heliocentric velocity of $+20.5 \pm 0.2 \text{ km s}^{-1}$. This is in excellent agreement with the value of $+20.4 \text{ km s}^{-1}$ found by Boggess et al. (1991) from GHRS data, but is significantly lower than the value of $+22 \text{ km s}^{-1}$ measured by Vidal-Madjar et al. (1986). It is important to determine whether or not this difference is significant, as its reality would imply temporal variation in the velocity of this component. As discussed in Section 2, the *internal* accuracy of our velocities, based on the fit to the Th–Ar comparison lines, is of the order of 0.05 km s^{-1} . In order to check that the UHRF velocities do not suffer from a large *systematic* error, we have compared the velocities of narrow interstellar molecular lines measured with this instrument towards the stars ζ Oph (Crawford et al. 1994) and ζ^1 Sco (S. K. Dunkin, personal communication) with those obtained independently with other instruments (Crawford 1989, 1990; Lambert, Sheffer & Crane 1990). These velocities all agree to within 0.4 km s^{-1} (0.1 km s^{-1} in the case of ζ^1 Sco). Thus we are confident that the 1.5 km s^{-1} velocity difference between this work and that of Vidal-Madjar et al. (1986) is not due to UHRF calibration errors. A more likely explanation is that variable substructure within this component causes the central velocity measured at lower resolution to change with time. We note that the extensive survey by Lagrange-Henri et al. (1992; their table 2) shows some evidence for a change in central velocity at the $\pm 1 \text{ km s}^{-1}$ level. Additional ultra-high-resolution observations will be needed to confirm this suggestion.

Our best-fitting Ca II column density for the main component ($\log N = 13.10$) is almost an order of magnitude higher than that obtained by Vidal-Madjar et al. (1986). This follows directly from our conclusion (Section 2.2) that this component is fully saturated (although we note that this circumstance also results in an order of magnitude uncertainty in the column density; cf. Table 1). Independent evidence that the column density of the main component is of the order of 10^{13} cm^{-2} comes from applying the doublet ratio method to the lower resolution observations of the H and K lines obtained previously by UCLES. The doublet ratio of 1.12 discussed in Section 2.2 implies a column density of $\log N = 13.08$, essentially identical to the value obtained here by line profile fitting. It is important to confirm this high Ca II column density, because it has significant consequences for the chemical abundances in the disc.

Based on a comparison of the Ca K and H lines, Lagrange-Henri et al. (1992) have determined that some of the material responsible for the redshifted variable features is clumped on scales smaller than the projected diameter of the star. If this is also the case for the features observed here, the column densities given in Table 1 will be underestimated. It would clearly be desirable to obtain UHRF data of both the K and H lines simultaneously, in order to quantify this effect further.

Finally, we note that the overall structure of the variable circumstellar Ca II profiles is similar to that found in the Fe II

Table 1. Line profile parameters for the circumstellar Ca II K absorption components in β Pic for the three dates of observation. Errors on the heliocentric radial velocities are typically ± 0.2 km s $^{-1}$.

May 11			Aug 26			Aug 29		
v_{helio}	b	Log N	v_{helio}	b	Log N	v_{helio}	b	Log N
(km s $^{-1}$)	(km s $^{-1}$)	(cm $^{-2}$)	(km s $^{-1}$)	(km s $^{-1}$)	(cm $^{-2}$)	(km s $^{-1}$)	(km s $^{-1}$)	(cm $^{-2}$)
....	14.2	$1.6^{+0.4}_{-0.2}$	$11.85^{+0.10}_{-0.15}$
....	15.8	$2.8^{+0.4}_{-0.3}$	$12.05^{+0.10}_{-0.05}$
16.8	$1.5^{+0.3}_{-0.3}$	$11.90^{+0.10}_{-0.10}$
20.5	$2.0^{+0.5}_{-0.7}$	$13.10^{+1.40}_{-0.50}$	20.5	$2.0^{+0.6}_{-0.7}$	$13.10^{+1.40}_{-0.50}$	20.6	$2.7^{+0.8}_{-0.5}$	$13.10^{+0.60}_{-0.30}$
27.3	$4.0^{+3.0}_{-2.0}$	$11.60^{+0.30}_{-0.30}$
33.4	$3.2^{+0.3}_{-0.2}$	$12.35^{+0.03}_{-0.10}$
43.7	$4.0^{+1.5}_{-0.5}$	$11.45^{+0.15}_{-0.10}$
....	48.0	$11.0^{+1.0}_{-2.0}$	$12.30^{+0.10}_{-0.10}$
....	49.0	$8.0^{+2.0}_{-2.0}$	$11.90^{+0.10}_{-0.15}$
50.7	$4.0^{+1.0}_{-2.0}$	$11.18^{+0.07}_{-0.48}$
....	70.3	$12.0^{+2.0}_{-2.5}$	$12.35^{+0.05}_{-0.10}$

lines by Boggess et al. (1991) using the GHRS on the *Hubble Space Telescope* (compare Fig. 1 of the present paper with their fig. 2). Boggess et al. suggested that the very broad redshifted components (such as we found to be present during August) may evolve from narrower features (such as that observed at $v_{\text{helio}} = 33.4$ km s $^{-1}$ on May 11). Such an evolution in the line profiles would be qualitatively consistent with the evaporation of infalling solid bodies (Lagrange-Henri et al. 1988), as the resulting ion clouds might be expected to develop wider velocity dispersions as they fall down the gravitational potential. It would clearly be of interest to test this hypothesis by using the unprecedented resolution of the UHRF to trace the evolution of these features over the course of several weeks.

ACKNOWLEDGMENTS

We thank the Director and staff of the Anglo-Australian Observatory for their strong support of the UHRF project. IAC thanks the Royal Society for the award of an Exchange Fellowship at the AAO, and the SERC for PDRA support. We thank Sarah Dunkin for providing the UHRF velocities of interstellar lines towards ζ^1 Sco.

REFERENCES

- Aumann H. H., 1984, BAAS, 16, 483
 Beust H., Lagrange-Henri A. M., Vidal-Madjar A., Ferlet R., 1989, A&A, 223, 304
 Beust H., Lagrange-Henri A. M., Vidal-Madjar A., Ferlet R., 1990, A&A, 236, 202
 Boggess A., Bruhweiler F. C., Grady C. A., Ebbets D. C., Kondo Y., Trafton L. M., Brandt J. C., Heap S. R., 1991, ApJ, 377, L49
 Crawford I. A., 1989, MNRAS, 241, 575
 Crawford I. A., 1990, MNRAS, 244, 646
 Crawford I. A., Barlow M. J., Diego F., Spyromilio J., 1994, MNRAS, 266, 903
 Diego F., 1993, Appl. Opt., 32, 6284
 Ferlet R., Hobbs L. M., Vidal-Madjar A., 1987, A&A, 185, 267
 Gledhill T. M., Scarrott S. M., Wolstencroft R. D., 1991, MNRAS, 252, 5p
 Golimowski D. A., Durrance S. T., Clampin M., 1993, ApJ, 411, L41
 Hobbs L. M., Vidal-Madjar A., Ferlet R., Albert C. E., Gry C., 1985, ApJ, 293, L29
 Hobbs L. M., Lagrange-Henri A. M., Ferlet R., Vidal-Madjar A., Welty D. E., 1988, ApJ, 334, L41
 Howarth I. D., Murray J., 1988, Starlink User Note No. 50
 Kondo Y., Bruhweiler F. C., 1985, ApJ, 291, L1
 Lagrange A. M., Ferlet R., Vidal-Madjar A., 1987, A&A, 173, 289
 Lagrange-Henri A. M., Vidal-Madjar A., Ferlet R., 1988, A&A, 190, 275
 Lagrange-Henri A. M., Gosset E., Beust H., Ferlet R., Vidal-Madjar A., 1992, A&A, 264, 637
 Lambert D. L., Sheffer Y., Crane P., 1990, ApJ, 359, L19
 Lecavelier des Etangs A. et al., 1993, A&A, 274, 877
 Paresce F., Burrows C., 1987, ApJ, 319, L23
 Shortridge K., 1988, Starlink User Note No. 86
 Smith B. A., Terrile R. J., 1984, Sci, 226, 1421
 Somerville W. B., 1988, Observatory, 108, 44
 Vidal-Madjar A., Hobbs L. M., Ferlet R., Gry C., Albert C. E., 1986, A&A, 167, 325